

**FAILURE ANALYSIS OF ULTRA-HIGH MOLECULAR WEIGHT
POLYETHYLENE ACETABULAR CUPS**

by

NICOLAAS DANIEL LOMBARD BURGER

Submitted in partial fulfilment of the requirements for the degree

DOCTOR PHILOSOPHIAE (PhD)

In Mechanical Engineering

In the

FACULTY OF ENGINEERING, THE BUILT ENVIRONMENT AND
INFORMATION TECHNOLOGY

UNIVERSITY OF PRETORIA
PRETORIA

DECEMBER 2005

Supervisors: Prof. PL de Vaal and Prof. J Meyer

ACKNOWLEDGEMENTS

I would like to thank the following people and companies for their support which made this study possible:

1. My Creator for giving me the ability to do this study
2. My wife Estelle and children for their support
3. Prof. E Fourie for his guidance
4. Prof. PL de Vaal for his assistance and guidance
5. Prof. J Meyer for his assistance and guidance
6. Mr At von Wielligh for his assistance in building the simulator
7. Mr F Bader, Department of Material Science, for his assistance with the microscopic work
8. Mr B Mans, Department of Biochemistry, for his assistance with the electrophoresis work
9. Dr F Weber, Sandton Clinic, for providing me with the samples
10. Messrs A Steynberg, T Opperman, T Wilcocks and A Hohls, postgraduate students for assistance with the test work
11. Gammatron (Pty) Ltd for the crosslinking and sterilisation of test pieces
12. CMTI Developments (Pty) Ltd for their financial assistance.

THESIS SUMMARY

Failure analysis of ultra-high molecular weight polyethylene acetabular cups

Student: Nicolaas Daniel Lombard Burger
Supervisors: Prof. PL de Vaal and Prof. J Meyer
Department: Mechanical and Aeronautical Engineering
University of Pretoria
Degree: PhD (Mechanical Engineering)
Keywords: Ultra-high molecular weight polyethylene, acetabular cup, wear, lubrication, poor heat conduction

Owing to the crippling nature of arthritis, surgeons have been trying for well over a century to successfully treat this debilitating disease particularly when attacking the hip joint. In the early 1970s, Sir John Charnley started with total hip replacement as a solution to this ever-increasing problem. Many different designs were developed but all the designs revolved around a femoral stem, femoral head and acetabular component. Independent of the design, longevity of the implant remains a problem. The major cause of replacements, according to various hip registers, is due to aseptic loosening resulting from osteolysis. According to these registers, the average in-vivo life of a hip replacement is approximately 12 years.

The main aim of this study was to determine the root cause of mechanical failure of the acetabular cups and to determine the origin of the excessive amount of ultra-high molecular weight polyethylene (UHMWPE) wear debris floating in the joint resulting in osteolysis.

During the study, various techniques were used to investigate the acetabular components to try to establish the root cause of mechanical failure. These techniques included:

1. Visual inspection
2. Investigation making use of dye penetrant spray
3. Investigation under stereo microscope
4. Investigation making use of a scanning electron microscope
5. Electrophoresis
6. Mass-spectrometric analysis
7. Analysis of the synovial fluid on high-frequency linear-oscillation machine (SRV).

The wear debris retrieved from the scar tissue surrounding the joints of a number of patients was also analysed.

Apart from the obvious defects such as mechanical damage due to impingement, the main defect on which this study focuses is the wear patches found on the inside of the acetabular components.

The wear areas were presented as areas where the surface layer of the UHMWPE was ripped off by adhering to the rotating femoral head. This type of failure is possible if localised overheating takes place resulting in the material either adhering to the rotating femoral head or the material being squeezed out under the prevailing pressure. Both these mechanisms were confirmed by the wear debris retrieved from the scar tissue, being either droplets of UHMWPE or whisker-like wear products.

To confirm the existence of elevated temperatures the brown discolouring on the inside of the acetabular cups was analysed, making use of electrophoresis, mass-spectrometric analysis and scanning electron microscope recordings. In this part of the study, it was confirmed that

localised temperatures on the bearing surface had reached at least 60°C during in-vivo service. This temperature was confirmed by inserting a thermocouple just under the surface of an acetabular cup and then measuring the temperature while in-vitro testing was taking place on a hip simulator.

The wear debris as retrieved was also duplicated in laboratory experiments while the temperature on the surface of an acetabular cup was monitored. It was established that wear particles similar in shape and size were formed at temperatures in excess of 90°C. At temperatures above 50°C the UHMWPE had visually shown extensive increase in creep, indicating that at these temperatures the material softens sufficiently for this type of debris to be generated

The overheating as described can also only occur if there is a lack of lubrication in the bearing couple. The synovial fluid from 12 patients was retrieved during revision surgery. This synovial fluid was then tested on a high-frequency linear-oscillation machine (Optimol SRV test machine) to determine the lubricity characteristics of the synovial fluid as retrieved. It was discovered that the load-carrying capability of the synovial fluid did not comply with the minimum requirements for a fluid to function as a lubricant.

The final conclusion of this study is that excessive amounts of wear debris are generated due to the localised overheating of the bearing couple as a result of insufficient lubrication. The localised heat build-up results in excessive amounts of wear debris being generated and deposited in the joint area resulting in osteolysis.

TABLE OF CONTENTS

	DESCRIPTION	PAGE
CHAPTER 1	INTRODUCTION	1
1.1	Development history of total hip replacement	1
1.2	Current concepts	4
1.3	Principal clinical diagnosis – total hip replacement	4
1.4	Clinical diagnosis resulting in revision hip replacement	6
1.5	Aim of study	10
CHAPTER 2	LITERATURE REVIEW	12
2.1	Introduction	12
2.2	Review of existing designs	13
2.2.1	Femoral component	14
2.2.2	Femoral head	15
2.2.3	Acetabular cup	16
2.3	Biomechanics of the hip joint	17
2.4	Material properties of ultra-high molecular weight polyethylene (UHMWPE)	23
2.5	Wear and wear modes in acetabular components	28
2.6	Summary of previous retrieval and wear studies	35
2.6.1	Summary of retrieval studies – excluding crosslinked components	35
2.6.2	Summary of follow-up study on crosslinked components (see paragraph 2.9 for the effects of crosslinking on the properties of UHMWPE.)	45
2.7	Results from simulator studies – in-vitro testing found in literature	46

2.8	Effects of gamma-irradiated sterilisation on wear characteristics	49
2.9	Effects of crosslinking on characteristics of UHMWPE	52
2.10	Hip simulators for in-vitro testing	55
2.11	Summary of literature review	62
CHAPTER 3	CREEP ANALYSIS FOR UHMWPE	63
3.1	Introduction	63
3.1.1	Test protocol	63
3.2	Clamping effects	64
3.2.1	Purpose of test	64
3.2.2	Test procedure	66
3.2.3	Results	68
3.3	Investigation of anisotropic effects	70
3.3.1	Purpose of test	70
3.3.2	Test procedure	70
3.3.3	Test results	72
3.4	Effect of elevated temperature on the creep properties of UHMWPE	74
3.4.1	Purpose of test	74
3.4.2	Test procedure	75
3.5	Effect of sterilisation on the creep properties of UHMWPE	77
3.5.1	Purpose of test	77
3.5.2	Test procedure	78
3.5.3	Test results	78
3.6	Effect of crosslinking on the creep characteristics of UHMWPE	81
3.6.1	Purpose of test	81
3.6.2	Test procedure	82

	3.6.3	Test results	82
	3.7	Proposed use of creep data in cup design	85
CHAPTER 4		PRELIMINARY INVESTIGATION OF RETRIEVED ACETABULAR CUPS	86
	4.1	Introduction	86
	4.2	Proposed failure criteria	88
	4.3	Descriptive explanation of defects in acetabular cups	88
	4.3.1	Mechanical damage	89
	4.3.2	Cracks in material	90
	4.3.3	Plastic flow	92
	4.3.4	Scratches	94
	4.3.5	Adhesion wear	94
	4.3.6	Wear particles embedded in base material	96
	4.3.7	Flaking	96
	4.4	Statistical analysis of retrieved acetabular cups	98
	4.5	Conclusion	100
CHAPTER 5		RETRIEVAL STUDY	101
	5.1	Introduction	101
	5.2	Summary of retrieved components	102
	5.3	Visual inspection of retrieved acetabular cups	103
	5.4	Inspection making use of dye penetrant	109
	5.5	Investigation making use of stereoscope	113
	5.6	Electron microscope investigation	119
	5.7	Electrophoresis	128
	5.7.1	Method	128
	5.7.2	Results	128
	5.8	Mass-spectrometric analysis	130

	5.8.1	Method	130
	5.8.2	Results	131
5.9		Analysis of wear particles from human tissue	132
	5.9.1	Method used	132
	5.9.2	Results	133
CHAPTER 6		FAILURE ANALYSIS OF RETRIEVED ACETABULAR COMPONENTS	137
	6.1	Introduction	137
	6.2	Cracks in acetabular components	137
	6.2.1	Cracks on the rim of the cup	137
	6.2.2	Cracks inside the bearing area	140
	6.3	Scratches	143
	6.3.1	Scratches caused by third-body wear	143
	6.3.2	Scratches formed by normal UHMWPE wear products	144
	6.4	Plastic flow	150
	6.5	Adhesion wear	152
	6.6	Postulate for mechanical failure of acetabular cups	156
CHAPTER 7		EXPERIMENTAL VERIFICATION	159
	7.1	Simulator studies	159
	7.1.1	Introduction	159
	7.1.2	Design of the simulator	161
	7.2	Overview of test work to be carried out	169
	7.3	Test with lubrication – test 1(a)	170
	7.3.1	Test protocol	170
	7.3.2	Test results	171
	7.4	Test without lubricant – test 1 (b)	173
	7.4.1	Test protocol	173
	7.4.2	Test results	173

7.5	Test to generate wear particles by generating frictional heat on the bearing surface – test 2 (a)	176
7.5.1	Purpose of the test	176
7.5.2	Test protocol	176
7.5.3	Test results	178
7.6	Test to generate wear particles by externally heating up a femoral head – test 2 (b)	181
7.6.1	Purpose of the test	181
7.6.2	Test protocol	181
7.6.3	Test results	182
7.7	Test to determine the coefficient of friction on the inside of an acetabular cup – test 3	185
7.7.1	Purpose of the test	185
7.7.2	Test protocol	185
7.7.3	Test results	187
7.8	Conclusion of experimental results	189
7.8.1	Simulator study	189
7.8.1.1	Temperature in acetabular cup	190
7.8.1.2	Wear debris retrieved from simulator	190
7.8.2	Simulating of wear debris formation in laboratory	194
7.9	Lubrication of the hip joint	197
CHAPTER 8	LUBRICATION OF THE HIP JOINT	198
8.1	Introduction	198
8.2	Apparatus used	201
8.3	Test method	203
8.4	Test outcome	205
8.5	Lubricity properties of patients	208
8.6	Discussion	209

CHAPTER 9	CONCLUSION AND RECOMMENDATIONS	212
9.1	Conclusion	212
9.2	Recommendations	214
	REFERENCES	217

LIST OF APPENDICES

ANNEXURE	DESCRIPTION
A	Retrieval analysis of 20 acetabular cups
B	Electron microscope analysis of white deposits in acetabular cups
C	Electron microscope investigation into brown discolouring in acetabular cups
D	Electron microscope investigation into brown discolouring in acetabular cups
E	Electron microscope investigation into micro wear
F	Electrophoresis analysis of particles retrieved from brown deposit in acetabular cups and synovial fluid
G	Mass spectrometric analysis of particles retrieved from brown deposit in acetabular cups and synovial fluid
H	Lubricity analysis of retrieved synovial fluid

LIST OF TABLES

Table		Page
Table 2.1	The maximum joint forces present in the hip joint, for a range of activities (Paul 1976)	21
Table 2.2	Mechanical properties of UHMWPE (Charnley, 1979; Material data sheet, Poli HiSolidur 1999 ; Lewis 2001)	27
Table 2.3	Summary of in-vivo wear rates as per literature from Jasty et al. (1997)	36
Table 2.4	Wear rates of metal -on- polyethylene total hip implants as summarised from bulk literature data (Buford & Goswani, 2004)	37
Table 2.5	Wear rates of ceramic -on- polyethylene total hip implants as summarised from bulk literature data (Buford & Goswani, 2004)	37
Table 2.6	Mean (mm or mm ³), standard deviation and range of wear measurements from retrieved acetabular components at revision surgery (Kesteris et al., 2003)	38
Table 2.7	Results of retrieval studies where wear was determined volumetrically (Sychterz et al., 1996; Jasty et al., 1997)	40
Table 2.8	Summary of sizes of wear particles as determined by Schmalzried et al. (1997) and Maloney et al. (1995)	44
Table 2.9	Summary of contemporary hip simulators (Calonius & Saikko, 2002)	57
Table 2.10	Variation with time of angular movement to be applied to the femoral test specimen (ISO 14242-1, 2002)	61
Table 3.1	Creep value differences for various test pieces	72
Table 3.2	Summary of creep values after 2 hours	77
Table 3.3	Summary of creep after gamma irradiation	81
Table 3.4	Summary of creep values after 2 hours	84
Table 4.1	The most common defects noticed on inside of retrieved cups	88

Table 4.2	Common defects present in acetabular cups with possible effect on useful life	97
Table 4.3	Statistical analysis of 47 retrieved cups, with in total 125 defects	99
Table 7.1	Values for masses needed to cause movement	187
Table 7.2	Values for estimated coefficient of friction under various conditions	189
Table 8.1	The test parameters used to determine the lubricity characteristics of the joint fluid	205
Table 8.2	Tests results to determine lubricity characteristics for 12 patients	208

LIST OF FIGURES

Figure	Page
Figure 1.1: Austin Moore prosthesis	2
Figure 1.2: The early prosthesis as designed by Sir John Charnley. Note the migration of the femoral head into the Teflon	3
Figure 1.3: Principle diagnosis - primary total hip replacements (Davidson et al., 2002; Davidson et al., 2003)	5
Figure 1.4: Schematic presentation of mechanism resulting in osteolysis (http://www.geocities.com/hip_replacements/history)	7
Figure 1.5: Wear debris-mediated osteolytic lesion superior (above) loose press-fit modular acetabular component. Note eccentricity of liner; mechanical failure ensued 5 years postoperatively (Dumbleton et al., 2002)	7
Figure 1.6: Polyethylene from an acetabular liner that has been attacked by the body, resulting in giant cells that eat away the bone resulting in component loosening (Manley et al., 2002)	7
Figure 1.7: Diagnosis - Revision surgery hip replacement (Davidson et al., 2002; Davidson et al., 2003)	8
Figure 1.8: Survival rate for different models of cemented and uncemented prostheses (Havelin et al., 2003)	9
Figure 2.1 Basic modular design of total hip replacement	13
Figure 2.2 Femoral osteolysis with signs of bone resorption below collar (Dumbleton et al., 2002).	15
Figure 2.3 Polyethylene liner with hydroxy-apatite-coated metal back (http://www.aesculap.de/)	17
Figure 2.4 Polyethylene liner in metal back with holes for fixation (http://www.depuy.com/)	17
Figure 2.5 Man standing on his right leg. The gravity vertical line from S ₆ falls in the supporting area of the right foot. The	18

weight G_5 is to be balanced in the right hip joint. M - abductor muscles of the right hip, R - hip resultant, S_5 - centre of gravity of the body mass to be borne in the right hip joint (Kummer, 1976)

Figure 2.6	Side (lateral) and back (posterior) view of abductor muscles (http://www.geocities.com/hip_replacements/history)	19
Figure 2.7	Side and back view of abductor forces acting on hip joint (http://www.geocities.com/hip_replacements/history)	19
Figure 2.8	Stress distribution on the normal hip joint (Kummer 1976)	20
Figure 2.9	Graphical presentation of the loading on the acetabular cup (Paul, 1976; Kummer, 1976; Sychterz et al., 1996; Zupanc et al., 2001)	20
Figure 2.10	Variation with time of hip joint forces for slow, normal and fast walking (Paul, 1976). The scale of the x axes is percentage time	21
Figure 2.11	Resultant force on hip joint for patient jogging on treadmill at 6 km/h (Bergmann et al. 1993; Bergmann et al. 1995). HS: heel strike, TO: toe off; MLR: measured load profile	22
Figure 2.12	PV values for UHMWPE at 20°C (Engineering Materials Handbook, 1987)	24
Figure 2.13	Izod impact strength against temperature with 15° double V notched (Engineering Materials Handbook, 1987)	25
Figure 2.14	Compression creep for various loads at 20°C (Engineering Materials Handbook, 1987)	26
Figure 2.15	The origins of the friction associated with the sliding of a hard, smooth surface over a polymer surface (Hutchings, 1992)	30
Figure 2.16	Wear rate of UHMWPE sliding against a steel counter face, as a function of the roughness of the steel surface (Hutchings, 1992)	33

Figure 2.17	Illustration of the asperities on the surface of a component after manufacturing (Hutchings, 1992)	33
Figure 2.18	Reduced contact area with increase in non-conformity between femoral head and acetabular cup	35
Figure 2.19	Linear wear in the cup and stem group (Kesteris et al., 2003)	38
Figure 2.20	Position of maximum wear in cups according to Sychterz et al. (1996)	40
Figure 2.21	Photograph of a polyethylene acetabular component (Jasty et al., 1997) retrieved during a revision that was performed because of osteolysis six years post-operatively. There is an eccentric pattern of wear. The superior worn area is highly polished and is separated from the inferior, less worn area by a ridge (small arrows). Note the evidence of impingement anteriorly (a large arrow). Discolouration and flaking are seen in the less worn area	42
Figure 2.22	Scanning electron micrograph showing the highly worn area with numerous multidirectional fine scratches in a well-fixed acetabular component that was retrieved at autopsy ten years after implantation (original magnification, x 79.5)	42
Figure 2.23	Scanning electron micrograph showing striations (arrows) perpendicular to the direction of the scratches, indicating tearing of the material during abrasive wear (original magnification, x 3900)	42
Figure 2.24	High-power scanning electron micrographs of a component retrieved six years after an arthroplasty. Reorganisation of the material has occurred during the wear process	43
Figure 2.25	X-ray that shows 2.5 mm wear in cup as indicated by	46

arrows as an eccentricity. No scale was shown in reference (Grobbelaar et al., 1999).

Figure 2.26	Particles of non-irradiated, ethylene oxide sterilised UHMWPE against chrome cobalt femoral head (x 10 000) (Ries et al., 2001)	49
Figure 2.27	Wear particles of inert gas gamma-irradiated UHMWPE against chrome cobalt (x 10 000) (Ries et al., 2001)	51
Figure 2.28	Average wear rate for acetabular components sterilised with gamma (Orishimo et al., 2003)	51
Figure 2.29	Average wear rate for acetabular components sterilised with ethylene oxide (Orishimo et al., 2003)	52
Figure 2.30	Tensile strength of crosslinked UHMWPE (Du Plessis et al., 1977)	53
Figure 2.31	Surface hardness of crosslinked UHMWPE (Du Plessis et al., 1977)	53
Figure 2.32	Impact energy of crosslinked UHMWPE (Du Plessis et al., 1977)	54
Figure 2.33	Wear particles of highly crosslinked UHMWPE subjected to 5 Mrad of gamma irradiation (x 10 000) (Ries et al., 2001)	55
Figure 2.34	Wear particles of highly crosslinked UHMWPE subjected to 10 Mrad of gamma irradiation (x 10 000) (Ries et al., 2001)	55
Figure 2.35	Boston hip simulator (http://www.geocities.com/hip_replacements/history)	56
Figure 2.36	Motion waveforms used in computation of slide tracks for hip simulators	57
Figure 2.37	Schematic illustration of the loading/motion configuration of the Bi-axial rocking motion (BRM) hip simulator (Wang et al., 1996)	58
Figure 2.38	Three-station, statically loaded bi-axial rocking motion	59

	(BRM) hip wear simulator (Saikko et al., 2001)	
Figure 2.39	Loading profile for hip simulator according to ISO standard (ISO 14242-1, 2002)	60
Figure 3.1	Illustration of clamping effect	65
Figure 3.2	Size of an ASTM test piece according to ASTM D2990 (1990)	65
Figure 3.3	Orientation of test pieces in virgin material	66
Figure 3.4a	Test set-up in Schenk testing machine	68
Figure 3.4b	Clip-on extensometer	68
Figure 3.5	Results for the test to determine clamping effect	69
Figure 3.6	Position and orientation of test piece 1 to 5	70
Figure 3.7	Position and orientation of test pieces 6 to 8	71
Figure 3.8	Creep in virgin material at different orientations	73
Figure 3.9	Orientation of test pieces machined from bar stock for tests at elevated temperatures	75
Figure 3.10	Test set-up for tests at elevated temperatures	76
Figure 3.11	Summary of creep results at elevated temperatures	76
Figure 3.12	Creep properties of material irradiated in air	79
Figure 3.13	Creep properties of material irradiated in nitrogen atmosphere	79
Figure 3.14	Creep properties of material radiated in air and heat treated at 80°C and tested at room temperature	80
Figure 3.15	Creep properties of crosslinked UHMWPE at room temperature	83
Figure 3.16	Creep properties of crosslinked UHMWPE tested at 50°C	83
Figure 3.17	Creep properties of crosslinked UHMWPE tested at 60°C	84
Figure 4.1	Mechanical damage on rim of cup	89
Figure 4.2	Schematic presentation of mechanical damage on rim of cup	89
Figure 4.3a	Metal-backed acetabular cup with cracks on rim	91
Figure 4.3b	Separation within material	91

Figure 4.4	Schematic layout of areas where cracks can be expected	92
Figure 4.5	Cup treated with dye penetrant showing “orange peel” effect indicating plastic flow of material	93
Figure 4.6	Schematic layout of expected plastic flow in acetabular cups	93
Figure 4.7	Scratches visible on inside of cup	94
Figure 4.8	Adhesion wear on inside made visible with dye penetrant treatment	95
Figure 4.9	Schematic layout of areas where cracks can be expected in the area under tensile stress	95
Figure 4.10	Acetabular cup with embedded PMMA particles	96
Figure 4.11	Acetabular cup with serious delamination visible	97
Figure 5.1	Fractured cup	102
Figure 5.2	A cup with delamination	103
Figure 5.3	Cross section of cups showing an amount of wear/creep	104
Figure 5.4	Deposited debris – coloured with liquid dye penetrant to make it more visible	104
Figure 5.5	Wear pattern in retrieved cups with area of debris deposits indicated	105
Figure 5.6	Crater in fractured cup	105
Figure 5.7	Cracking in fractured cup	106
Figure 5.8	A cup with evidence of interference and subsequent damage	106
Figure 5.9	Piece of steel embedded in polyethylene (magnification x 40)	107
Figure 5.10	Plastic flow on the rim of cup	108
Figure 5.11	Amount of plastic flow	108
Figure 5.12	White deposits on inside of cup and brown discolouring	109
Figure 5.13	Deposited debris, resulting flow pattern and adhesion wear	110
Figure 5.14	The rim of cup showing plastic flow on circumference of	110

	rim	
Figure 5.15	A cup with areas of higher concentration of debris	111
Figure 5.16	Close-up of the area of adhesion wear	112
Figure 5.17	Schematic lay-out to indicate position of fretting mark	112
Figure 5.18	Magnification (x 10) of defect before treatment with dye penetrant	113
Figure 5.19	Magnification (x 20) of defect before treatment with dye penetrant	113
Figure 5.20	Magnification(x 20) of defect after treatment with dye penetrant	114
Figure 5.21	Magnification (x 40) of second crater after treatment with dye penetrant	114
Figure 5.22	Magnification (x 10) of defect on rim of cup	115
Figure 5.23	Magnification (x 20) of defect on rim of cup	115
Figure 5.24	Magnification (x 10). From this photograph the white irregular shape of material deposited is clearly visible	116
Figure 5.25	Magnification (x 20). The arrow points to a droplet of material which was either extruded from the bearing surface or was flattened after being ripped out of the surface	116
Figure 5.26	Magnification (x 20). The photograph shows softened/extruded debris with what looks like craters in between. Note the irregular shape of the deposit after being flattened by the ball	117
Figure 5.27a	Magnification (x 40): The results from Figure 5.25 are investigated further. It can be seen that the white piece of material appears not to have been totally removed from the base material, as there are no sharp edges on one side	117
Figure 5.27b	Schematic of material extruded from the bearing surface	117
Figure 5.28	Magnification (x 20) of wear area on bearing surface	118

Figure 5.29	Magnification (x 40) of wear on bearing surface area	118
Figure 5.30	Electron microscope investigation of a brown layer on inside of cup (magnification x 50)	119
Figure 5.31	Electron microscope investigation of the brown layer on inside of the cup (magnification x 250)	120
Figure 5.32	Electron microscope image of virgin UHMWPE sample (magnification x 10 000)	120
Figure 5.33	An electron microscope image of deformed UHMWPE (magnification x 10 000)	120
Figure 5.34	Anatomical cup orientation with position of worn area	121
Figure 5.35	Machining marks visible in acetabular cup	122
Figure 5.36	Machining marks on inside of cup (magnification x 500)	122
Figure 5.37	Wear particle entrapped in cup (magnification x 3700)	122
Figure 5.38	Surface of acetabular cup with scratches due to third-body wear (magnification x 1500)	123
Figure 5.39	Abrasion wear on acetabular cup (magnification x 1300)	123
Figure 5.40	Back scatter analysis on wear particle lodged at end of abrasion wear in acetabular cup (magnification x 1500)	124
Figure 5.41	Adhesion wear area in acetabular cup	125
Figure 5.42	Electron microscope photograph of adhesion wear in acetabular cup (magnification x 23)	125
Figure 5.43	Adhesion wear area under higher magnification (magnification x 5000)	125
Figure 5.44	Adhesion wear defect under electron microscope (magnification x 22)	126
Figure 5.45	Adhesion wear under higher magnification (magnification x 190)	126
Figure 5.46	Acetabular cup with visible plastic flow on bearing area (magnification x 180)	127
Figure 5.47	Plastic flow on bearing area under higher magnification (magnification x 1300)	127

Figure 5.48	Electrophoresis analysis of synovial fluid and retrieved proteins from acetabular cups	129
Figure 5.49	Mass-spectrometric analysis of a synovial fluid sample	132
Figure 5.50	Schematic explanation of formation of jagged/wavy edges during extrusion	134
Figure 5.51	Particles retrieved from tissue (magnification x 40)	134
Figure 5.52	Retrieved particle (magnification x 100)	134
Figure 5.53	Retrieved particle (magnification x 40)	135
Figure 5.54	Retrieved particle (magnification x 100)	135
Figure 6.1	Metal-back acetabular cup with cracks and delamination on rim of cup	138
Figure 6.2	Cross section of acetabular cup showing delamination on the rim of the cup (magnification x 20)	138
Figure 6.3	Schematic layout of UHMWPE liner not fitting snugly into metal backing	139
Figure 6.4	Acetabular component after catastrophic failure	140
Figure 6.5	Crack on inside of acetabular cup	141
Figure 6.6	Electron microscope analysis of adhesion wear area (magnification x 110)	141
Figure 6.7	Crater under the surface after adhesion wear (magnification x 450)	142
Figure 6.8	Acetabular cup with severe scratches on inside	143
Figure 6.9	Acetabular cup with multidirectional fine scratches and with machining marks still visible (magnification x 20)	144
Figure 6.10	Bearing area with signs of big scratches and area with adhesion wear	145
Figure 6.11	Scratches on bearing surface with white particles visible (magnification x 35)	146
Figure 6.12	Scratch mark on bearing surface (magnification x 250)	146
Figure 6.13	Final position of particle causing damage to bearing surface (magnification x 1500)	147

Figure 6.14	Electron microscope back scatter analysis of scratch (magnification x 1500)	147
Figure 6.15	Scratch on bearing surface (magnification x 33)	148
Figure 6.16	End of scratch on bearing surface (magnification x 1300)	148
Figure 6.17	Whisker-like debris retrieved from patient (magnification x 20)	149
Figure 6.18	Debris retrieved from patient (magnification x 40)	149
Figure 6.19	Plastic flow of material visible in cup (magnification x 10)	151
Figure 6.20	Plastic flow in acetabular cup (magnification x 1300)	152
Figure 6.21	Area with plastic flow lines visible (magnification x 75)	152
Figure 6.22	Visible adhesion wear in acetabular cup	153
Figure 6.23	Butterfly wear pattern on inside of acetabular cup	153
Figure 6.24	Area with adhesion wear (magnification x 40)	153
Figure 6.25	Area with adhesion wear exposing the base material of the acetabular cup (magnification x 5000)	154
Figure 6.26	Wear particle with smaller particles attached to it (magnification x 3700)	155
Figure 6.27	Area with adhesion wear (magnification x 60)	155
Figure 6.28	Adhesion particle about to be broken out (magnification x 200)	156
Figure 6.29	Steps in wear debris formation in acetabular cup	158
Figure 7.1	Concept for simulator movement	162
Figure 7.2a	Schematic layout of the simulator	163
Figure 7.2b	Schematic layout of the simulator: Side view	163
Figure 7.3	Hip movement as measured by Bergman et al. (1993)	164
Figure 7.4	Recorded force/time graph of the simulator	164
Figure 7.5	Loading spring with adjusting plate	165
Figure 7.6	Assembly of stabilising springs	165
Figure 7.7	Graphical presentation of the forces on the connecting pin	166
Figure 7.8	Mechanical stops to achieve $\pm 5^\circ$ abduction/adduction	167

	rotation	
Figure 7.9	Two cups in position showing the thermocouples and strain gages	168
Figure 7.10	Detail of the acetabular cup in the test station	168
Figure 7.11	Test-recording equipment	171
Figure 7.12	Wear particles on filter material (magnification x 40)	172
Figure 7.13	Wear particle retrieved from simulator (magnification x 100)	172
Figure 7.14	Retrieved wear particle from simulator (magnification x 900)	173
Figure 7.15	Wear surface on the inside of the cup (magnification x 10)	174
Figure 7.16	Wear on inside of a cup (magnification x 20)	174
Figure 7.17	Wear debris retrieved from an acetabular cup on simulator (magnification x 20)	175
Figure 7.18	Wear debris retrieved from an unlubricated acetabular cup in a hip simulator (magnification x 40)	175
Figure 7.19	Wear debris retrieved from an unlubricated acetabular cup in a hip simulator (magnification x 40)	176
Figure 7.20	Test layout to manufacture wear particles with frictional heat	177
Figure 7.21	Area of damage on a test piece	178
Figure 7.22	Surface damage on UHMWPE test piece (magnification x 20)	178
Figure 7.23	Wear debris adhering to femoral ball - indicated with an arrow	179
Figure 7.24	Wear debris generated by frictional heat at a measured temperature of 105°C (magnification x 40)	179
Figure 7.25	Wear particle at higher magnification (magnification x 100).	180
Figure 7.26	Schematic layout of surface roughness	181
Figure 7.27	Surface of a test piece after damage by preheated	182

	femoral head (magnification x 10)	
Figure 7.28	Damage surface of UHMWPE test piece (magnification x 20)	182
Figure 7.29	Wear particles adhering to femoral ball —indicated with an arrow	183
Figure 7.30	Retrieved wear debris from preheated ball test. Ball temperature 100°C (magnification x 20)	183
Figure 7.31	Wear particles retrieved from externally heated femoral head at temperature of 100°C (magnification x 40)	184
Figure 7.32	Wear particles retrieved from externally heated femoral head at a temperature of 100°C (magnification x 40)	184
Figure 7.33	Test set up for determining coefficient of friction between ceramic femoral head and UHMWPE acetabular cup	186
Figure 7.34	Data used for the calculation of coefficient of friction	188
Figure 7.35	Wear debris retrieved from simulator (magnification x 100)	191
Figure 7.36	UHMWPE wear debris retrieved from scar tissue (magnification x 100)	192
Figure 7.37	UHMWPE wear particle still attached to base material (magnification x 3700)	192
Figure 7.38	UHMWPE wear debris retrieved from simulator running without lubrication (magnification x 20)	193
Figure 7.39	UHMWPE wear debris retrieved from scar tissue (magnification x 100)	193
Figure 7.40	UHMWPE wear particle generated by means of frictional heating (magnification x 100)	195
Figure 7.41	UHMWPE wear debris generated by preheating the femoral head (magnification x 40)	195
Figure 7.42	UHMWPE wear debris retrieved from scar tissue (magnification x 100)	196
Figure 8.1	A schematic drawing of the human hip joint	198

	(http://www.healthsystem.virginia.edu/UVAHealth/adult_arthritis/anatomy.cfm)	
Figure 8.2	Areolar tissue (magnification x 400) (http://science.nhmccd.edu/biol/tissue/areolar.html)	199
Figure 8.3	Schematic layout of surface roughness.	201
Figure 8.4	Schematic layout of the Optimol SRV machine	202
Figure 8.5	Fixed specimen in Optimol SRV machine	203
Figure 8.6	Moving specimen in Optimol SRV machine	203
Figure 8.7	An example of a typical lubricity test result. The loads at failure are indicated on the graph	206
Figure 8.8	Wear scar on moving specimen (ball)	207
Figure 8.9	Wear scar on fixed specimen (disk) (magnification x 60)	207
Figure 8.10	Combined lubricity data for 12 patients as tested with averages as indicated	209
Figure 8.11	Adhesion wear on bearing surface of retrieved acetabular cup	210
Figure 8.12	Wear particle still attached to UHMWPE acetabular cup	210
Figure 8.13	Wear debris retrieved from patient no. 5 (magnification x 200)	211

List of symbols

- σ Principal stress – either tension or compression
- r Radius
- E Young's modulus of elasticity
- H Hardness of material
- ν Poisson's ratio

Glossary

Abduction	Act of turning outward.
Acetal	Acetal, also known as polyacetal, polyoxymethylene (POM), or polyformaldehyde, is a high-performance engineering polymer.
Adduction	Act of turning inward.
Arthritis	Arthritis is inflammation of one or more joints. When joints are inflamed they can develop stiffness, warmth, swelling, redness and pain. There are over 100 types of arthritis, including osteoarthritis, rheumatoid arthritis, ankylosing spondylitis, psoriatic arthritis, lupus, gout, and pseudogout. Earlier and accurate diagnosis can help to prevent irreversible damage and disability.
Arthrodesis	Athrodesis is the surgical fixation of a joint. It is also called artificial ankylosis.
Avascular necrosis	Condition in which poor blood supply to an area of bone leads to bone death. This is called avascular necrosis and osteonecrosis.
Cortical bone	Main construction of the shaft of the femur.
Dislocation, congenital hip	The abnormal formation of the hip joint in which the ball at the top of the thigh bone (the femoral head) is not stable within the socket (the acetabulum). The ligaments of the hip joint may also be loose and stretched.
Dysplasia	Abnormal in form. Dysplasia is derived from the Greek <i>dys-</i> (bad, disordered, abnormal) and <i>plassein</i> (to form). For example, retinal dysplasia is the abnormal formation of the retina during embryonic development.

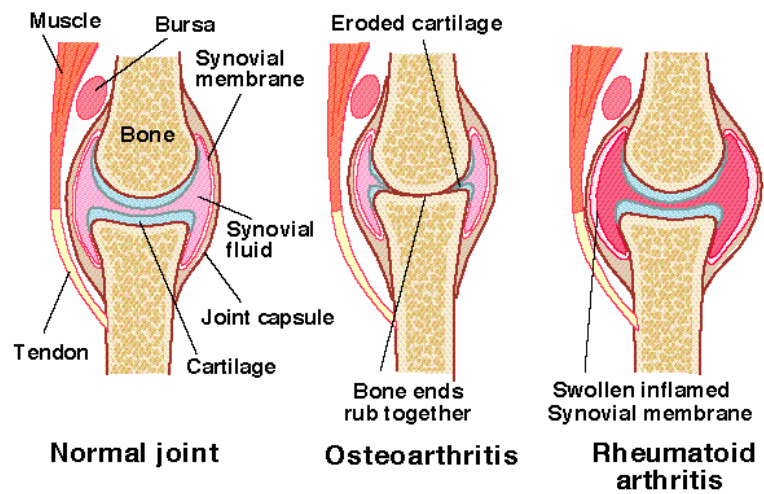
xxx

Electrophoresis	Gel electrophoresis is a method that separates macromolecules — either nucleic acids or proteins — on the basis of size, electric charge, and other physical properties.
Ethylene oxide	Ethylene oxide is a colourless liquefied gas with a sweet odour used for the sterilisation of implants and equipment within a steriliser/autoclave.
Extension	Movement that increases the angle at a joint.
Fixation, internal	A surgical procedure that stabilises and joins the ends of fractured (broken) bones by mechanical devices, such as metal plates, pins, rods, wires or screws.
Flexion	Movement that decreases the angle at a joint.
Fracture	A fracture is a break in the bone or cartilage. It usually is a result of trauma. A fracture can, however, be the result of an acquired bone disease such as osteoporosis or the result of abnormal formation of bone in a congenital bone disease such as osteogenesis imperfecta ("brittle bone disease").
Hydroxy-apatite	Plasma-sprayed calcium phosphate coating that is bio-active.
Izod impact strength	Material test that provides toughness data under dynamic rather than static conditions (Shigley & Mischke, 2003).
Lateral	Side of the patient.
Lysis	Destruction. Haemolysis (<i>haemo-lysis</i>) is the destruction of red blood cells with the release of haemoglobin; bacteriolysis (<i>bacterio-lysis</i>) is the destruction of bacteria; and so on. Lysis can also refer to the subsidence of one or

more symptoms of an acute disease as, for example, the fever of pneumonia.

Osteoarthritis

A type of arthritis caused by inflammation, breakdown, and eventual loss of cartilage in the joints. Osteoarthritis is also known as degenerative arthritis. Osteoarthritis can be caused by ageing, heredity, and injury from trauma or disease. The most common symptom of osteoarthritis is pain in the affected joint(s) after repetitive use.

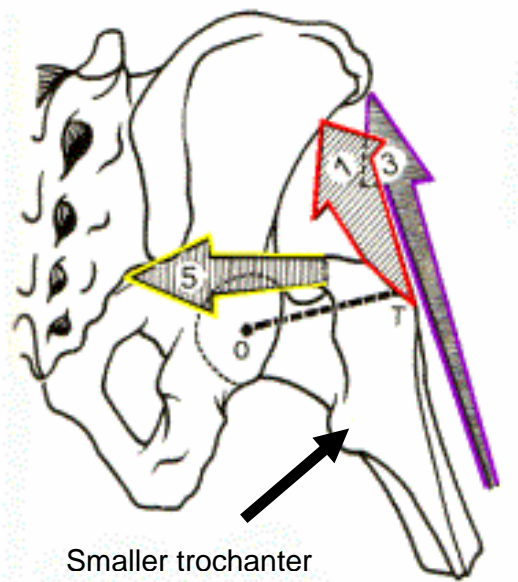


NORMAL and ARTHRITIC JOINTS *A Bonnell*

Osteolastic

A pathological condition resulting from accumulation of acid or a loss of base in the body; characterised by an increase in hydrogen ion concentration (decrease in pH). Has various causes including several states that produce excesses in various acids; included are diabetes mellitus (ketone bodies), renal insufficiency (phosphorus, sulfuric and hydrochloric acids), respiratory disease (carbonic acid), and prolonged strenuous exercise (lactic acid).

Osteolysis	Also called particle disease, aggressive granulomatosis. Particulate debris from wear of arthroplasty components, most commonly polyethylene component (Schmalzried et al.,1997). Large pieces sequestered in fibrous tissue.
Osteotomy	Osteotomy is an operation in which a bone is cut, enabling a surgeon to reposition it. An osteotomy may be performed to lengthen or shorten a leg, to correct bowed or bent legs, or to reset a fracture.
PMMA	Polymethyl methacrylate — a thermoplastic polymer synthesised from methyl methacrylate and used as bone cement for the fixation of implant.
Smaller trochanter	



Posterior	Back of the patient.
Rheumatoid arthritis	An auto-immune disease that causes chronic inflammation of the joints, the tissue around

the joints, as well as other organs in the body. Auto-immune diseases occur when the body tissues are mistakenly attacked by its own immune system. The immune system is a complex organisation of cells and antibodies designed normally to "seek and destroy" invaders of the body, particularly infections. Patients with these diseases have antibodies in their blood which target their own body tissues, where they can be associated with inflammation. Because it can affect multiple other organs of the body, rheumatoid arthritis is referred to as a systemic illness and is sometimes called rheumatoid disease. While rheumatoid arthritis is a chronic illness (meaning it can last for years), patients may experience long periods without symptoms.